Continental Shelf Research ∎ (∎∎∎∎) ∎∎∎–∎∎∎

Contents lists available at SciVerse ScienceDirect

Continental Shelf Research

journal homepage: www.elsevier.com/locate/csr

Research papers

A multi-method approach for benthic habitat mapping of shallow coastal areas with high-resolution multibeam data

Aaron Micallef [a,b,*], Timothy P. Le Bas [c], Veerle A.I. Huvenne [c], Philippe Blondel [d], Veit Hühnerbach [c], Alan Deidun [a]

[a] University of Malta, Msida, MSD 2080, Malta
[b] GRC Geociències Marines, Facultat de Geologia, Universitat de Barcelona, Spain
[c] National Oceanography Centre, European Way, Southampton, SO14 3ZH, UK
[d] Department of Physics, University of Bath, Bath, BA2 7AY, UK

ARTICLE INFO

Article history:
Received 30 July 2011
Received in revised form
15 March 2012
Accepted 19 March 2012

Keywords:
Habitat mapping
Multibeam bathymetry
Multibeam backscatter
Coastal waters
Maltese Islands

ABSTRACT

The coastal waters of the Maltese Islands, central Mediterranean Sea, sustain a diversity of marine habitats and support a wide range of human activities. The islands' shallow waters are characterised by a paucity of hydrographic and marine geo-environmental data, which is problematic in view of the requirements of the Maltese Islands to assess the state of their coastal waters by 2012 as part of the EU Marine Strategy Directive. Multibeam echosounder (MBES) systems are today recognised as one of the most effective tools to map the seafloor, although the quantitative characterisation of MBES data for seafloor and habitat mapping is still an underdeveloped field. The purpose of this study is to outline a semi-automated, Geographic Information System-based methodology to map the distribution of habitats in shallow coastal waters using high-resolution MBES data. What distinguishes our methodology from those proposed in previous studies is the combination of a suite of geomorphometric and textural analytical techniques to map specific types of seafloor morphologies and compositions; the selection of the techniques is based on identifying which geophysical parameter would be influenced by the seabed type under consideration.

We tested our approach in a 28 km^2 area of Maltese coastal waters. Three data sets were collected from this study area: (i) MBES bathymetry and backscatter data; (ii) Remotely Operated Vehicle imagery and (iii) photographs and sediment samples from dive surveys. The seabed was classified into five elementary morphological zones and features – flat and sloping zones, crests, depressions and breaks of slope – using morphometric derivatives, the Bathymetric Position Index and geomorphometric mapping. Segmentation of the study area into seagrass-covered and unvegetated seafloor was based on roughness estimation. Further subdivision of these classes into the four predominant types of composition – medium sand, maërl associated with sand and gravel, seagrass settled on sand and gravel, and seagrass settled on bedrock – was carried out through supervised classifications of morphometric derivatives of the bathymetry and textural indices of backscatter, based on information from training stations. The resulting morphologic and seabed composition maps were combined to plot the distribution of the predominant habitats in the coastal waters offshore NE Malta, some of which are of high conservation value. Ground-truthing of the habitat map using ROV imagery and dive observations confirms that our approach produces a simplified and accurate representation of seafloor habitats while using all the information available within the MBES data sets.

1. Introduction

Shallow coastal zones represent some of the most productive environments of the ocean and are characterised by complex mosaics of benthic habitats (Eyre and Maher, 2011; Gray, 1997). Knowledge of the spatial distribution, quality and quantity of these habitats is fundamental to our understanding of marine ecosystems and our ability to protect them from anthropogenic impacts (Jackson et al., 2001). Habitat maps have thus become a major tool in the assessment and monitoring of coastal marine systems, as well as in marine spatial planning, resource assessment and offshore engineering.

Historically, seafloor classification has largely been based on the collection of physical samples and divers' observations. In the last

* Corresponding author at:University of Malta, Msida, MSD 2080, Malta. Tel.: +356 99051124.
E-mail address: aaron.micallef@um.edu.mt (A. Micallef).

0278-4343/$ - see front matter © 2012 Elsevier Ltd. All rights reserved.
http://dx.doi.org/10.1016/j.csr.2012.03.008

two decades, multibeam echosounder systems (MBES) have gained broad acceptance as a means to map large areas of the seafloor and delineate them into geological and geomorphological regions (Kostylev et al., 2001; Todd et al., 1999), to map the distribution of biological systems (Kostylev et al., 2003; McGonigle et al., 2009) and to identify archaeological components (Singh et al., 2000). The reasons for the increased popularity of MBES are numerous. First, MBES provide continuous acoustic coverage of large swathes of the seafloor; in comparison, sampling and diving cover significantly smaller areas and are therefore less cost effective (Kenny et al., 2003). Second, recent developments in marine acoustic technology have allowed MBES to match or supersede other types of conventional acoustic survey systems (e.g., single beam echosounder, side scan sonar) as a mapping tool (Brown and Blondel, 2009). This is particularly the case for multibeam backscatter data, which today give as much, or more, detail than is available with side scan sonar systems alone (Le Bas and Huvenne, 2009). The possibility of collecting high-resolution bathymetric and backscatter data simultaneously has thus led to a preference of MBES over side scan sonar as a marine mapping tool (Brown et al., 2011).

Seabed geology, in particular topography and composition, is known to influence benthic community structure and ecological processes at many spatial scales (Bourget et al., 1994; Cusson and Bourget, 1997; Guichard and Bourget, 1998; Kostylev et al., 2001; Snelgrove and Butman, 1994) and is becoming an important component of seabed and habitat mapping programs (e.g., Cochrane and Lafferty, 2002). Conventionally, segmentation of MBES data sets into seabed geological features has been carried out manually (e.g., Todd et al., 1999). Manual segmentation is inherently subjective, slow and potentially inaccurate (Cutter Jr et al., 2003), which is problematic in view of the subtle variations that may be present in acoustic responses, the large volumes of data being collected during modern surveys, and the increase in seabed mapping programmes worldwide (Blondel and Gómez Sichi, 2009). There is thus a need to develop quantitative, computational techniques that are robust, accurate and unbiased (Cutter Jr et al., 2003). These techniques should rapidly transform large areas of spatially-complex bathymetric and backscatter data into simple, easily-visualised maps that supplement the interpreter with as much information as possible. Mitchell and Clarke (1994) were among the first to quantitatively characterise seabed geology using both bathymetric and backscatter data. The quantitative classification of MBES data is an advancing field, and several different approaches are currently under development and reported in the literature (e.g., Erdey-Heydorn, 2008; Lamarche et al., 2011; Marsh and Brown, 2009; Wright and Heyman, 2008).

The coastal waters of the Maltese Islands, Mediterranean Sea, are characterised by a paucity of detailed hydrographic and marine geo-environmental data. This is problematic in view of the requirement of the Maltese Islands to implement the regulations associated with the European Union Marine Strategy Framework Directive by July 2012. The Marine Strategy Framework Directive requires member states to carry out an initial assessment of the environmental status of their marine waters. Among the characteristics required to fulfil this initial assessment are: (i) topography and bathymetry of the seabed, (ii) predominant seabed and water column habitat type(s) with a description of the characteristic physical and chemical features, such as depth, structure and substrata composition of the seabed. Considering that Maltese coastal waters are also prone to various types of anthropogenic impacts, there is an urgent need to develop tools for the rapid and accurate mapping of the Maltese seabed and to produce good quality maps of its shallow seabed habitats.

The objectives of our study are therefore to: (i) outline a quantitative, semi-automated method to map the distribution of seafloor composition and morphology; and (ii) to test the applicability of this method in shallow coastal waters. We carry this out using high-resolution multibeam bathymetry and backscatter data, together with precisely-geolocated Remotely Operated Vehicle (ROV) imagery, dive observations and seabed samples, acquired offshore the Maltese Islands.

2. Regional setting

The Maltese archipelago is situated in the central Mediterranean Sea, between Italy and North Africa, and consists of Malta, Gozo, Comino and a number of small uninhabited islets (Fig. 1(a)). The islands are composed of a series of Tertiary massive coralline limestones and fine-grained biomicrites with intercalated beds of phosphorite nodules and clays (Pedley et al., 1976). This layered sequence is intensely disrupted by an Early Miocene to mid-Pliocene NE–SW trending fault set, and a Late Pliocene NW–SE trending fault system. The seabed around the Maltese Islands is one of the least studied areas in Europe, although recent studies are showing that this region hosts important geological (e.g., fluid flow structures (Micallef et al., 2011)) and biological (e.g., white coral communities (Freiwald et al., 2009)) systems. The Maltese Islands are located at the south-western edge of the Malta Plateau, a shallow, north–south striking ridge that links the Maltese Islands with Sicily (Fig. 1(a)). The seabed topography

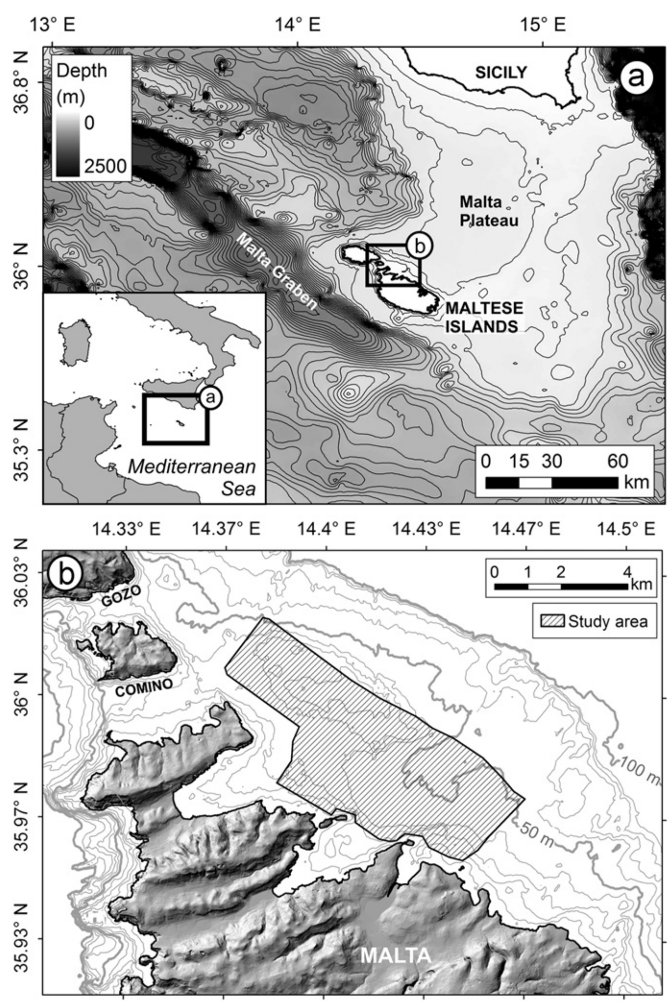

Fig. 1. (a) Bathymetric map of the central Mediterranean Sea showing the location of the Maltese Islands (isobaths at 50 m intervals). *Source*: Smith and Sandwell (1997); (b) Bathymetric map of the Maltese coastal waters (shallower than 100 m; isobaths at 10 m intervals), with the study area denoted by a black hatched polygon (source: Malta Maritime Authority; the bathymetric map should not be used for navigation purposes).

Please cite this article as: Micallef, A., et al., A multi-method approach for benthic habitat mapping of shallow coastal areas with high-resolution multibeam data. Continental Shelf Research (2012), http://dx.doi.org/10.1016/j.csr.2012.03.008

between Sicily and the Maltese Islands is generally shallow (mean depth of 115 m) and gently sloping. The archipelago also straddles the northern rim of the Malta Graben, a NW–SE oriented graben that has been active since the Late Miocene (Reuther and Eisbacher, 1985). The seabed to the south-west of the Maltese Islands is thus steeper and much deeper (> 1000 m).

In this study we investigate a $\sim$28 km^2 area of seabed located to the north-east of the coastline of Malta, where the water depth varies between 6 and 57 m (Fig. 1(b)). This study area has been selected for two reasons. First, the area is known to host a variety of seabed morphologies and substrate types (e.g., Borg et al., 2009; Sciberras et al., 2009), making it an ideal site to assess the effectiveness of our technique. Second, the study area falls within a Special Area of Conservation of International Importance (MT0000105) under the EC Habitats Directive, which has been recently designated within Maltese coastal waters to protect the extensive meadows of *Posidonia oceanica* (*L.*) Delile located in the area. *Posidonia oceanica* is a seagrass species endemic to the Mediterranean Sea. Meadows of *Posidonia oceanica* constitute the most important ecosystems in the Mediterranean Sea because they oxygenate the water column, stabilise the seabed, provide shelter to 20–25% of Mediterranean species, and are sites of high rates of primary production and organic material deposition (Boudouresque and Meinesz, 1982; Pergent-Martini and Le Ravallec, 2007). The study area is, however, still prone to extensive human disturbance — it includes a popular tourist area and dense urban settlements on shore, and busy recreational boating routes, vessel bunkering zones, a fish farm and sites earmarked for a potential wind farm and aquaculture zone offshore. The need to improve the spatial and environmental management of the study area is thus urgent.

3. Data sets

Our study is based on three data sets acquired between October 2009 and August 2011.

The first data set was collected during a MBES survey aboard the R/V Hercules using a hull-mounted Kongsberg-Simrad EM-3002D system operating at a frequency of 300 kHz. A total of 290 km of tracks were run at an average speed of 6.5 knots. The average swath width was $\sim$100 m, and a swath overlap of 10–50% was maintained. Positional data were provided by a Trimble DSM 132 differential Global Positioning System (dGPS). Sound velocity profiles were taken at the deepest point every day of the survey. Both bathymetry and backscatter data were derived from the MBES survey (Fig. 2). The bathymetry data were processed with CARIS Hydrographic Information Processing System (HIPS) by accounting for sound velocity variations, tides and basic quality control. The backscatter data were processed with PRISM (Processing of Remotely-sensed Imagery for Seafloor Mapping) software (Le Bas and Hühnerbach, 1998). Processing included radiometric corrections, geometric corrections and mosaicking. Bathymetric and backscatter data were exported as 32-bit rasters with a cell size of 1 m.

The second data set includes underwater video surveys of ten seabed sites carried out from the R/V Hercules (Fig. 2(b)). High-definition digital video imagery was acquired using a SeaEye Panther Plus Remotely Operated Vehicle (ROV) from a total area of 0.036 km^2 of seabed. Positional information was obtained from an Ultra-Short Baseline transponder relative to the ship's position.

The third data set consists of visual observations of main physical features and seabed composition, photographs and sediment samples obtained from seven sites during boat-based diving surveys (Fig. 2(b)). Positional information was determined with buoys and dGPS. The sediment samples were collected using a small shovel and analysed for grain size distribution using a Coulter-Counter LS230 Laser Particle Size Analyser.

The ROV and diving sites were selected to encompass all the principal textures identified from the backscatter data. Dive sites A–F and ROV site G were used as training sites to ground-truth backscatter textures, whereas ROV sites 1–9 and dive site 10 were used as test sites to validate the results of our proposed methodology (Fig. 2(b)).

4. Method

Our habitat mapping approach combines a suite of techniques that segment the acquired MBES data in terms of seabed morphology and composition (Fig. 3).

4.1. Seabed morphology

We classify the bathymetric data into five morphological zones and features — flat and sloping zones, crests, depressions and breaks of slope; these are the most elementary and prevalent morphological units identified within the study area via a 3D visualisation of the bathymetric data.

4.1.1. Flat and sloping zones

The study area was first classified into flat and sloping zones. We applied a low pass 3×3 cell filter to the bathymetric data using the Filter tool in ArcGIS™ to reduce the influence of small-scale irregularities. A map of slope gradient, which is a measure of the maximum rate of elevation change from one cell to its neighbour across 3×3 cell neighbourhoods, was then extracted using the equation:

$$\text{Slope gradient} = \arctan(p^2+q^2)^{1/2} \tag{1}$$

where $p=\partial z/\partial x$; $q=\partial z/\partial y$ (x=longitude; y=latitude; z=depth; all in metres).

We plotted the cumulative frequency distribution curve for the slope gradient values across the study area; the point of inflection occurs at a slope gradient value of 5° (Fig. 4(b)). When mapped, this value separates flat to very gentle seafloor from more prominent morphologies, such as escarpments (in agreement with Micallef et al. (2007) and Erdey-Heydorn (2008)). The slope gradient map was therefore reclassified as flat (seabed with a slope gradient between 0° and 5°) or sloping (seabed with a slope gradient higher than 5°) using the Reclassify tool in ArcGIS™ (Fig. 3 and Fig. 4(a)).

4.1.2. Crests and depressions

To extract crests and depression across the study area we used the Bathymetric Position Index (BPI). BPI is a second-order derivative of bathymetry based on the Topographic Position Index (TPI) (Weiss, 2001), which was adapted for seafloor studies by Lundblad et al. (2006). The BPI algorithm uses a neighbourhood analysis function to evaluate the elevation differences between a focal point and the mean elevation of the surrounding cells within a user-defined shape. A negative BPI value represents a cell that is lower than its neighbouring cells (i.e., depression), whereas a positive value represents a cell that is higher (i.e., crest). Flat areas and areas of constant slope produce near-zero values. The BPI algorithm was implemented in ArcGIS™ using a raster calculator and the Focal statistics mean tool (which calculates the mean value for a specified neighbour shape and size) on the bathymetric data set. An annulus with an inner radius of 1 m and an outer radius of 5 m was used; the average depth value calculated for the outer 5 m radius was then subtracted from the average depth value within the inner 1-m radius circle for each cell. These radii were selected to identify crests/depressions that are at least 10 m in width. To allow comparison of our results with those of studies that have classified the seabed using BPI, the BPI data

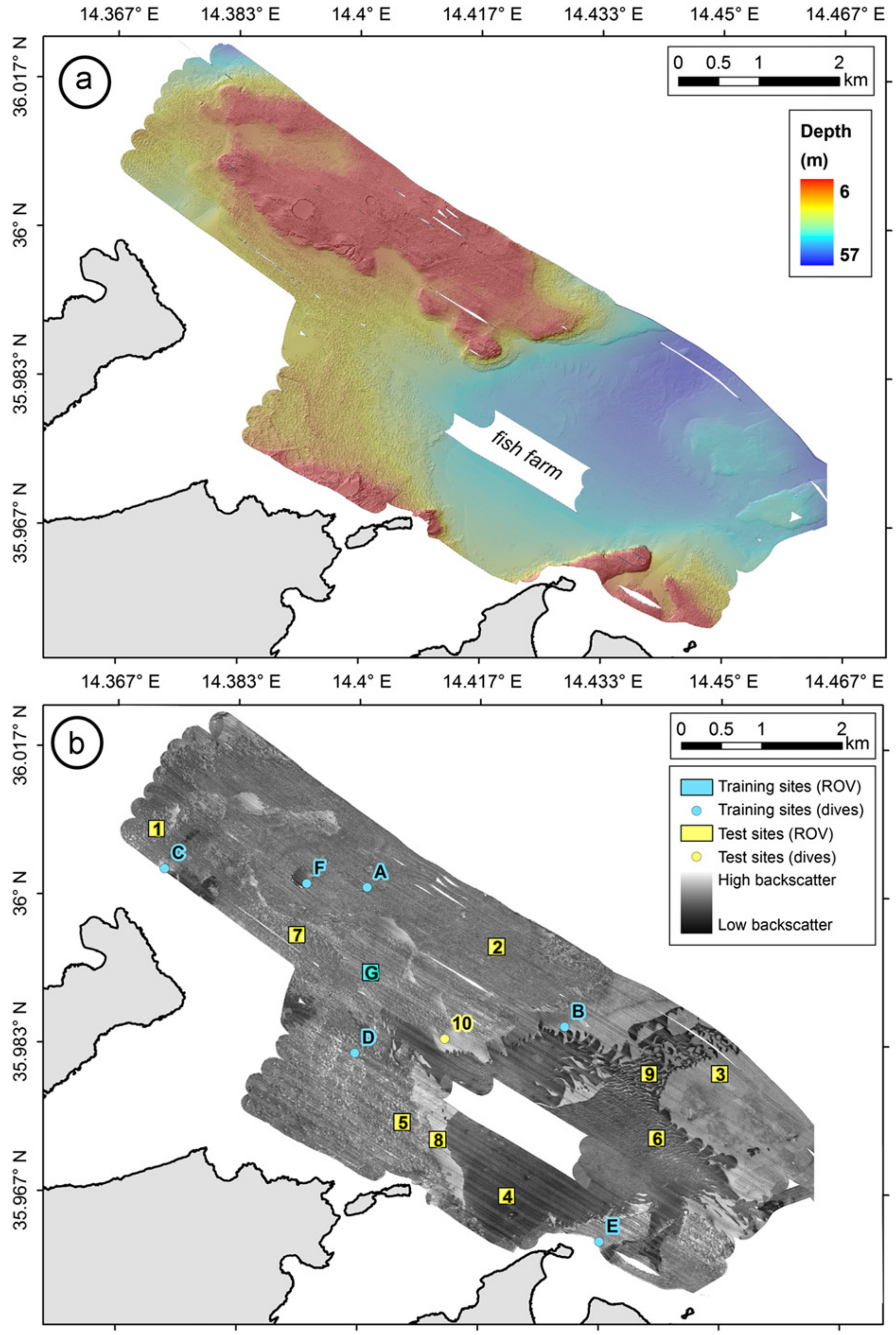

Fig. 2. Processed (a) bathymetric data draped on a shaded relief map and (b) backscatter data, acquired from the study area. The location of the seven training sites and ten test sites are denoted in Fig. (b).

were standardised. This was carried out by subtracting the mean value of the BPI data from each BPI data point and dividing by the standard deviation; in this way, the mean BPI had a value of 0 and the standard deviation had a value of $-1/+1$. The standardised value of each data point was then multiplied by 100 (Erdey-Heydorn, 2008). Using the Reclassify tool, standardised BPI data higher than 100 were classified as crests, whereas those lower than -100 were classified as depressions (Fig. 3 and Fig. 4(c)).

4.1.3. Breaks of slope

Certain morphological features of geological interest, such as faults, fissures and steep escarpments, consist of lineaments, discontinuities or boundaries that are not identified by zonal classifications. For this reason, we extracted a geomorphometric map of the study area to delineate breaks of slope, which we define as changes in slope gradient between adjacent cells that are higher than 60° (Micallef et al., 2007). This was carried out by first computing a profile curvature map of the study area across 3×3 cell neighbourhoods using the equation:

$$\text{Profile curvature} = -(p^2 r + 2pqs + q^2 t)/[(p^2+q^2)(1+p^2+q^2)^{3/2}] \tag{2}$$

where $p = \partial z/\partial x$; $q = \partial z/\partial y$; $r = \partial^2 z/\partial x^2$; $s = \partial^2 z/\partial x \partial y$; $t = \partial^2 z/\partial y^2$

Profile curvature represents the maximum change in slope gradient between adjacent cells. The profile curvature map was then reclassified into two intervals ($>60^\circ\ \text{m}^{-1}$ for convex breaks of slope and $<-60^\circ\ \text{m}^{-1}$ for concave breaks of slope) using the

Please cite this article as: Micallef, A., et al., A multi-method approach for benthic habitat mapping of shallow coastal areas with high-resolution multibeam data. Continental Shelf Research (2012), http://dx.doi.org/10.1016/j.csr.2012.03.008

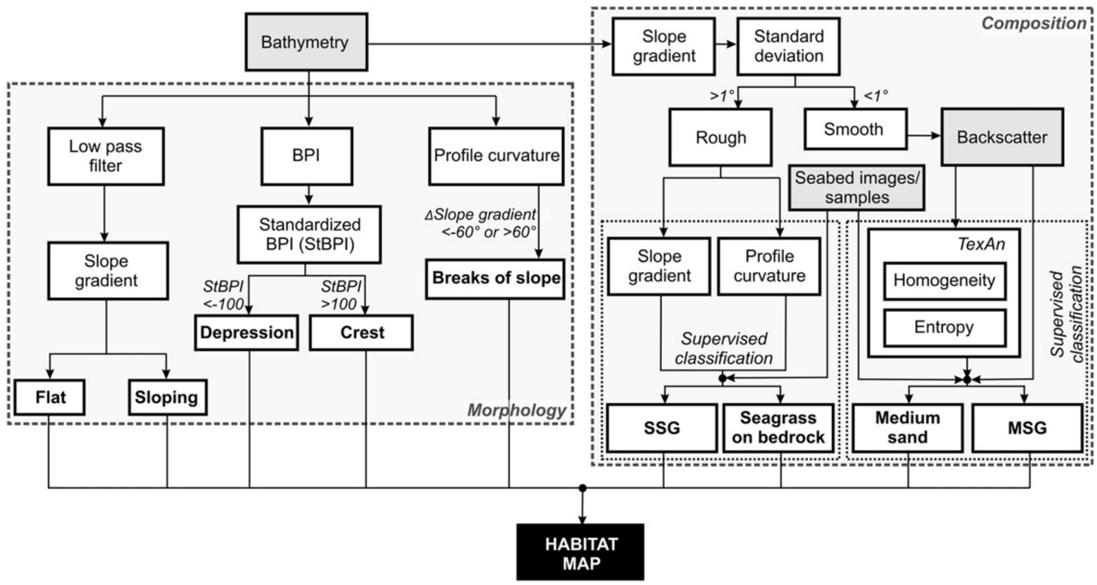

Fig. 3. Flowchart of the methodology used in this study. (BPI=Bathymetric Position Index; SSG=seagrass settled on sand and gravel; MSG=maërl associated with sand and gravel).

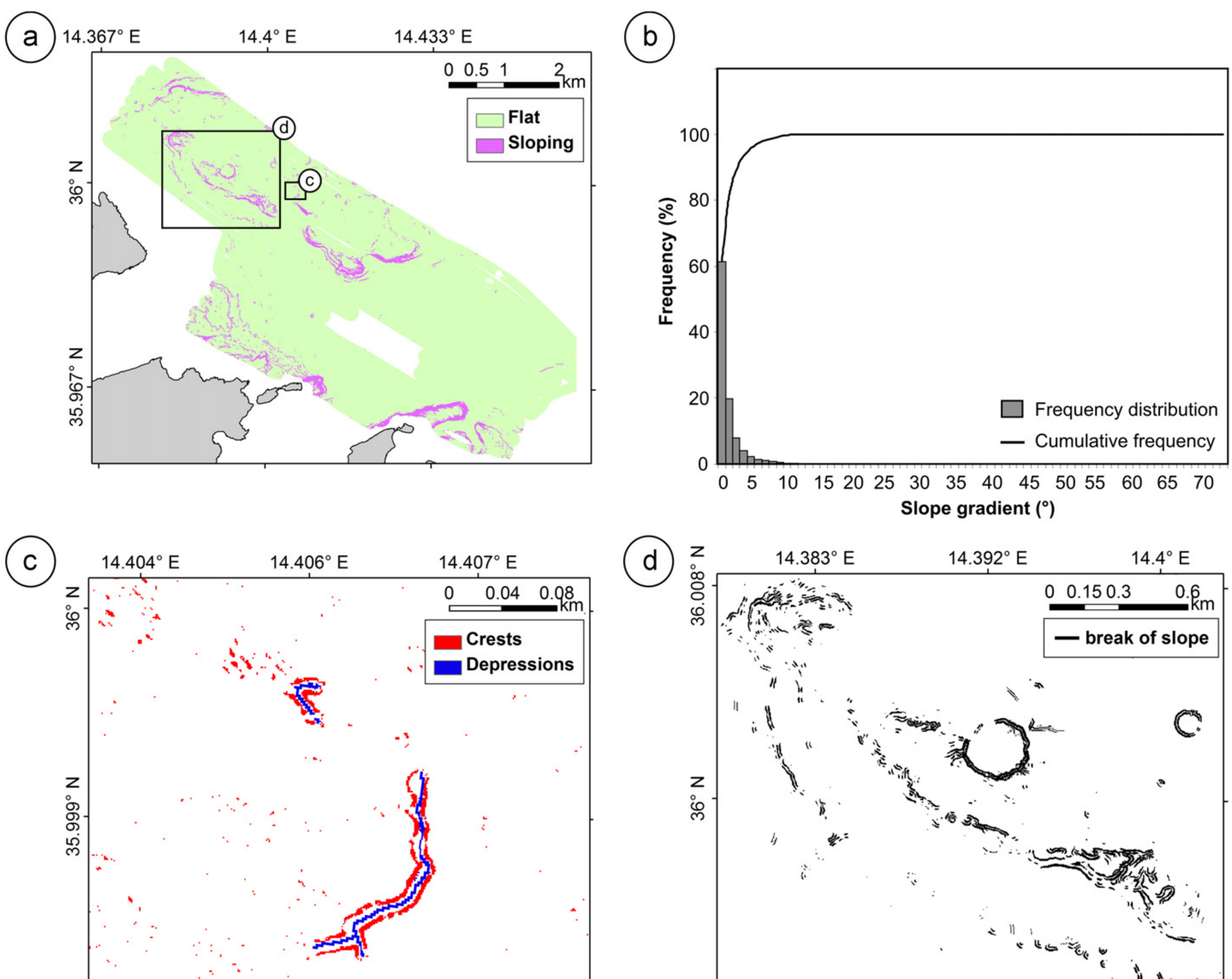

Fig. 4. (a) Classification of the study area into flat and sloping zones. (b) Frequency distribution histogram and cumulative frequency distribution curve for slope gradient values across the study area. (c) Enlarged section of the map of extracted crests and depressions, showing two irregular, channel-like features. (d) Enlarged section of the map of extracted breaks of slope. The locations of Figs. (c) and (d) are shown in Fig. (a).

Reclassify tool. These two intervals were mapped as lineaments using the Contour tool in ArcGIS™. This method is described in more detail in Micallef et al. (2007).

4.2. Seabed composition

Segmentation of the seabed according to surficial composition entails a combination of morphometric and textural analyses of both bathymetric and backscatter data.

4.2.1. Seabed composition classes

To identify the different types of seabed composition across the study area we took into consideration the seabed photographs and sediment samples from the training sites (Fig. 2(b); Fig. 5). Sediment samples were divided into different classes according to their median grain size distribution (d_{50}) and the Wentworth scale (Wentworth, 1922). We interpreted four main classes of seabed composition, in accordance with the marine habitats proposed for the Maltese Islands as aligned with the habitat classification system adopted within the EU Habitats Directive (Borg and Schembri, 2002). These classes include:

(i) Medium sand (habitat III.3.3 Biocoenosis of coarse sands and muddy heterogeneous sediment);
(ii) Maërl associated with sand and gravel (habitat III.3.2 Biocoenosis of coarse sand and fine gravels under the influence of bottom currents);
(iii) Seagrass settled on sand and gravel (habitat III.5.1 Biocoenosis of *Posidonia oceanica* meadows); and
(iv) Seagrass settled on bedrock (habitat III.5.1 Biocoenosis of *Posidonia oceanica* meadows).

These four classes are associated with characteristic backscatter intensities and textures at the seven training sites, as shown in Fig. 5. The sand and gravel classes mainly comprise fragmented biogenic material, in particular carbonate shells. Maërl is typical of the circalittoral zone and consists of accumulations of loose, living or dead, coralline algae (Bosence, 1979). It forms two types of sediment — maërl facies with free living red algal branches, and 'facies à pralines' dominated by rhodoliths; these facies are generally associated with bioclastic sediments derived from carbonate fragments reworked in the mobile substrate (Pérès and Picard, 1964). Since maërl beds serve as feeding ground for many species and are associated with high biodiversity levels, they are listed in Annex V of the Habitats Directive as of community interest. The class of 'maërl associated with sand and gravel' comprises maërl and rhodolith fragments and reworked bioclastic sediments derived from these beds. The seagrass classes predominantly encompass *Posidonia oceanica* meadows, which are listed as a priority natural habitat in Annex I of EC Directive 92/43/EEC on the Conservation of Natural Habitats and of Wild Fauna and Flora (Hemminga and Duarte, 2000). These seagrass habitats may included matte, which is a construction resulting from horizontal and vertical growth of *Posidonia oceanica* rhizomes with entangled roots and entrapped sediment (Francour et al., 2006). The class of 'seagrass settled on bedrock' is not always spatially continuous and may include small areas of unvegetated bedrock in places.

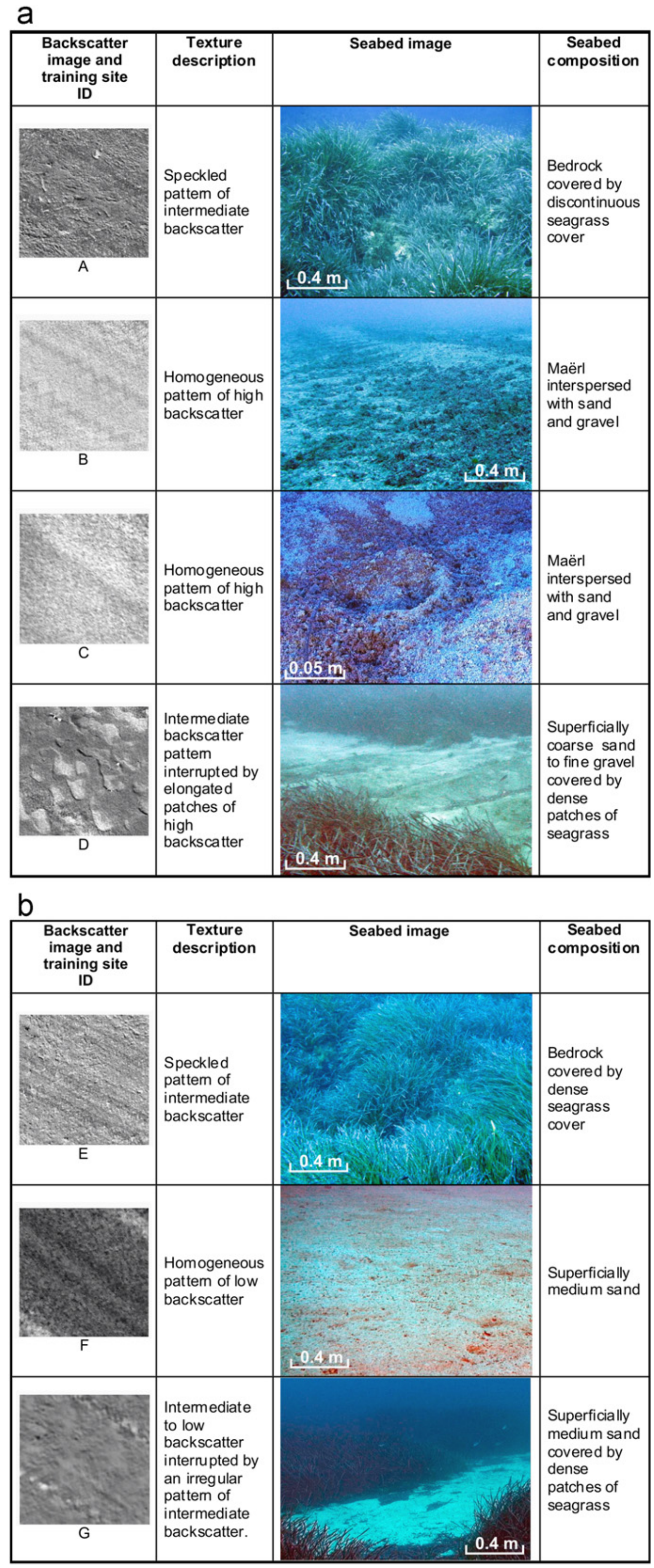

Fig. 5. Backscatter imagery (200 × 200 m) and description of backscatter textures at the seven training sites (locations shown in Fig. 2(b)). High backscatter is represented by light colours, low backscatter by dark colours. A representative seabed photograph and the interpreted seabed composition (from seabed imagery and samples) are also included.

4.2.2. Seabed segmentation based on roughness

Backscatter strength is primarily a function of the topography at the sediment-water interface, while the intrinsic acoustic reflectivity of the seabed (e.g., composition) is a secondary contributor (Jackson and Richardson, 2007). Reducing the influence of topographic roughness on backscatter intensity facilitates classification of backscatter data according to seabed composition. We therefore classified the bathymetric data into different roughness zones in order to segment each roughness zone into seabed composition classes separately. We extracted a slope gradient map from the bathymetric data by calculating slope gradient values across 3×3 cell neighbourhoods using Eq. (1). We used this map to generate a standard deviation of slope gradient map by calculating the standard deviation of slope gradient values across 3×3 cell neighbourhoods using the Block statistics tool in in ArcGIS™, as proposed in Micallef et al. (2007). Using the standard deviation of slope gradient map, the seabed was divided into smooth and rough zones according to a visually-selected threshold of 1° (Fig. 6(a)); this value discriminates between areas of unvegetated seabed (smooth zones with a standard deviation of slope gradient $<1°$) from seagrass covered seabed (rough zones with a standard deviation of slope gradient $>1°$) (Fig. 5 and Fig. 6(a)).

4.2.3. Classification of seabed into composition classes

We utilised two different methods to classify the seabed into the four main composition classes.

4.2.3.1. Unvegetated seabed (smooth zones): textural analyses and supervised classification. The training sites indicate that the unvegetated, smooth zones of seabed predominantly comprise medium sand or maërl associated with sand and gravel. We segment the backscatter data in the smooth zones into these two classes using textural analyses. In sonar imagery classification, texture refers to the distribution of acoustic energy and their positions relative to each other (Blondel, 1996; Blondel and Gómez Sichi, 2009). Textural analyses quantitatively describe the grey levels and their spatial relationships in small windows throughout an image. Grey Level Co-occurrence Matrices (GLCMs) have been shown to be the most adaptable tools for textural analyses of sonar imagery (Blondel, 1996; 2000; Gao et al., 1998). Numerically, the GLCMs express the relative frequency of occurrence $P_D(i,j)$ of two points, with respective grey levels i and j, at a Euclidean distance D from each other (D is the inter-pixel displacement). Two textural indices, entropy and homogeneity, are sufficient to describe the GLCMs and resolve most textures visible in sonar imagery (Blondel, 1996; Blondel and

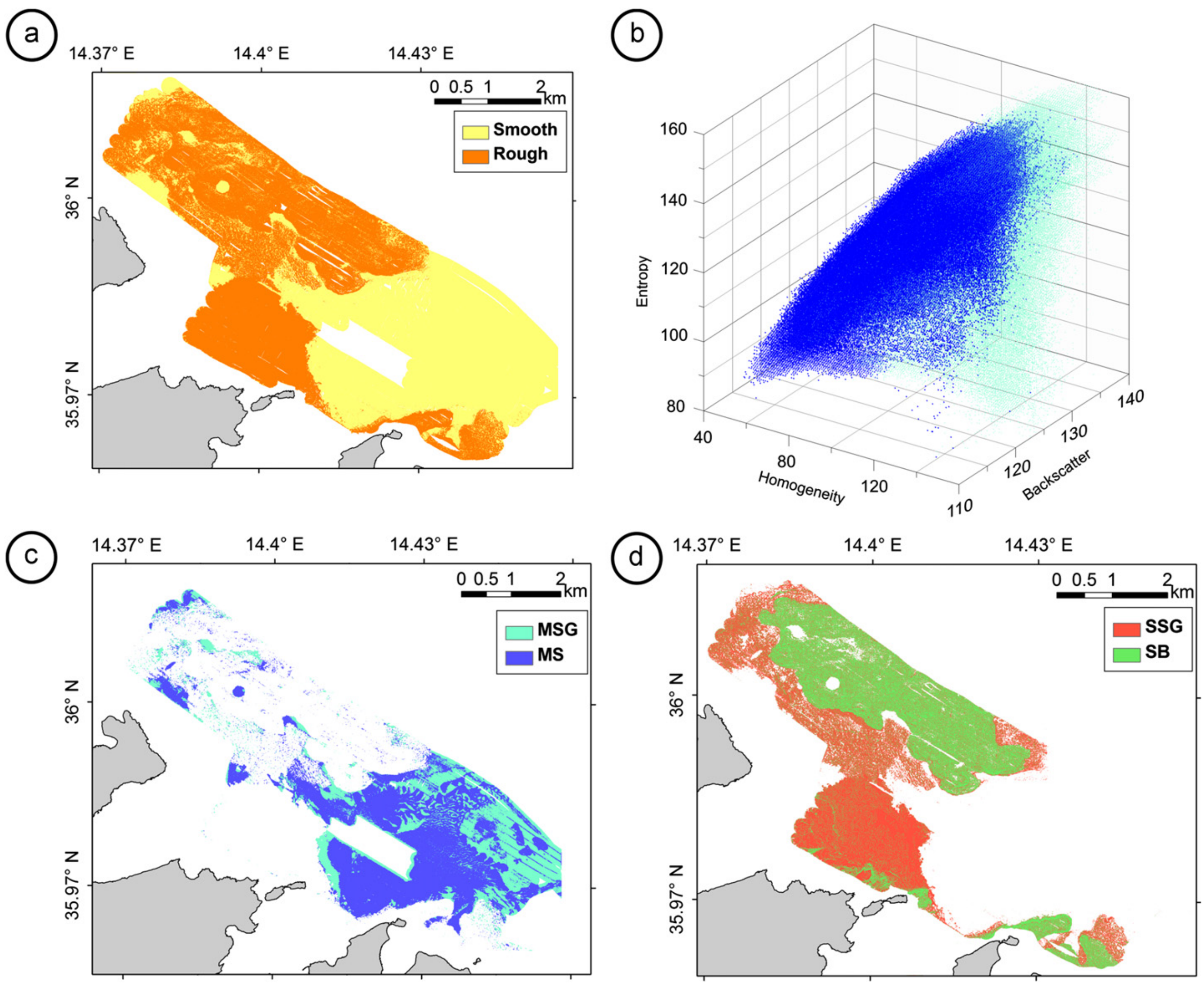

Fig. 6. (a) Classification of bathymetric data into smooth and rough zones based on the standard deviation of slope gradient. (b) 3D feature space graph of medium sand (dark blue) and maërl associated with sand and gravel classes (light blue) in terms of backscatter, homogeneity and entropy. (c) Supervised classification map of smooth zones into two classes: medium sand and maërl associated with sand and gravel. (d) Supervised classification map of rough zones into two classes: seagrass settled on sand and gravel, and seagrass settled on bedrock. (MS=medium sand; MSG=maërl associated with sand and gravel; SSG=seagrass settled on sand and gravel; SB=seagrass settled on bedrock). (For interpretation of the references to colour in this figure legend, the reader is referred to the web version of this article.)

Please cite this article as: Micallef, A., et al., A multi-method approach for benthic habitat mapping of shallow coastal areas with high-resolution multibeam data. Continental Shelf Research (2012), http://dx.doi.org/10.1016/j.csr.2012.03.008

Gómez Sichi, 2009; Blondel et al., 1998). Entropy measures the lack of spatial organisation inside the computation window, whereas homogeneity quantifies the amount of local similarities inside the computation window (Blondel, 1996). Writing NG as the number of grey levels in the image, entropy and homogeneity are computed as follows:

$$\text{Entropy} = -\sum_{i=1}^{NG}\sum_{j=1}^{NG}(P_D(i,j)\times \log_{19} P_D(i,j)) \tag{3}$$

$$\text{Homogeneity} = \sum_{i=1}^{NG}\sum_{j=1}^{NG}\left(\frac{P_D(i,j)}{1+(i-(j/K))^2}\right) \tag{4}$$

The factor K was first used by Shokr (1991) and Blondel (1996) to ensure invariance during linear grey level transformation:

$$K = \frac{\sum_{i=1}^{NG}\sum_{j=1}^{NG}|i-j|\times P_D(i,j)}{\sum_{i=1}^{NG}\sum_{j=1}^{NG}P_D(i,j)} \tag{5}$$

These textural values were then normalised on 8 bits to smooth out small variations of no physical significance (Blondel, 1996; 2000). Entropy and homogeneity indices were calculated for various values of the number of grey levels NG (from $NG=8$, by increasing powers of 2 until $NG=256$, corresponding to the full dynamic range of the sonar image), the window size (from 10×10 to 80×80 pixels, by increasing steps of 10 pixels) and the inter-pixel displacement D (from 5 pixels within the computation window, to its maximum size minus 5 pixels, by increasing steps of 10 pixels). All combinations were computed and the results were plotted with backscatter intensity until the points for the class of medium sand were separated from the points for the class of maërl associated with sand and gravel in an entropy-homogeneity-backscatter graph (Fig. 6(b)). This occurred when a minimum of 32 grey levels was used with a window size of 50×50 pixels and an inter-pixel displacement of 10 pixels. Maps of entropy and homogeneity were generated using these parameters. To ensure that the textural indices are not significantly influenced by the angle of ensonification, the co-occurrence matrices were averaged for angles of 0°, 45°, 90° and 135°, in accordance with Reed and Hussong (1989) and Blondel (1996). Classification signature files, storing the multivariate statistics (means, variance and covariance) for entropy, homogeneity and backscatter intensity, were generated for the two classes of seabed composition using data from the training sites using the Create signatures tool (Fig. 5(a)) 10 m diameter circle around each training site was used to collect these data. Supervised classification of the three rasters was carried out using a maximum-likelihood classifier, which is a clustering algorithm in ArcGIS™ that assigns each cell in the rasters to one of the classes represented in the signature file. This is carried out by computing the probability for each class to determine the membership of the cells to the class and producing a grid of classes in the form of a raster thematic map The class of medium sand is characterised by lower mean and covariance values of backscatter intensity, homogeneity and entropy than the class of maërl associated with sand and gravel (Fig. 6(b)). Textural analyses was carried out using the software TexAn (Blondel, 2000).

4.2.3.2. Seagrass covered seabed (rough zones): morphometric attributes and supervised classification. Rough zones consist predominantly of seagrass settled on sand and gravel, and seagrass settled on bedrock. The backscatter texture for these two classes of seabed composition does not differ significantly, which means that the seagrass cover contributes most to these textures, in agreement with observations by De Falco et al. (2010). This is expected at high multibeam frequencies, as used in this study, because they do not allow high penetration into the seabed. On the other hand, the distribution of seagrass seems to be directly influenced by the underlying substrate, resulting in discernibly different patterns in the bathymetry data set for seagrass settled on sand and gravel and seagrass settled on bedrock. Thus, we used bathymetric data to classify the rough zones into these two classes (Fig. 3). We used the slope gradient and profile curvatures maps, computed in Sections 4.1.3 and 4.2.2, respectively, to generate classification signature files with the multivariate statistics (means, variance and covariance) of profile curvature and slope gradient; data were obtained from a 10 m diameter circle at the training sites for areas of rough seabed. Based on the classification signature files, a maximum likelihood classification was carried out to classify the bathymetric data into seagrass settled on sand and gravel and seagrass settled on bedrock, and generate the thematic map in Fig. 6(d). The class of seagrass on bedrock is characterised by higher mean and covariance values of slope gradient and profile curvature than the class of seagrass settled on sand and gravel.

4.3. Generation of habitat map

The resulting seabed morphology and composition maps (Fig. 4(a), (c); Fig. 6(c) and (d) were combined into a single habitat map using the Combine function in ArcGIS™, which combines multiple rasters so that a unique output value is assigned to each unique combination of input values. These maps were also slightly smoothed to eliminate small and isolated areas that do not translate well to actual habitat information and that are possibly misclassified. ArcGIS™ tools Boundary clean (which cleans ragged edges between classes by shrinking and expanding them) and Majority filter (which replaces cells in a raster based on the majority of their contiguous neighbouring cells) were used to carry out the smoothing. In this way, each cell in our study area was classified in terms of morphology and composition. The break of slope map (Fig. 4(d)) was finally overlaid on the final habitat map (Fig. 7).

5. Results

5.1. Shallow water habitats offshore NE Malta

The predominant habitats offshore NE Malta are extents of medium sand, maërl associated with sand and gravel, seagrass settled on sand and gravel, and seagrass settled on bedrock, all located on flat areas (Fig. 7). Other classes are considerably less abundant. The majority of the study area is covered by unvegetated medium sand, which is predominantly located in the southern half of the study area. The eastern boundaries of this habitat are characterised by an intricate pattern of lobes and ripples that are positive in relief and that are adjacent to, and occasionally cover, the maërl habitat (Fig. 8(b)). The latter is prevalently interspersed with sand and gravel.

The seabed above ∼40 m depth is largely dominated by different *Posidonia oceanica* ecomorphoses. Most of the seagrass is settled on sand and gravel between Sikka l-Bajda (a shallow, elongated, NW–SE trending limestone reef) and the NE coast of Malta (Fig. 7). The rest of the seagrass is settled on bedrock; this habitat is mainly located in the northern half of the study area on the Sikka l-Bajda reef, or close to the shoreline (Fra Ben), where peninsulas have become submerged (Figs. 7 and 8(c)). The surface

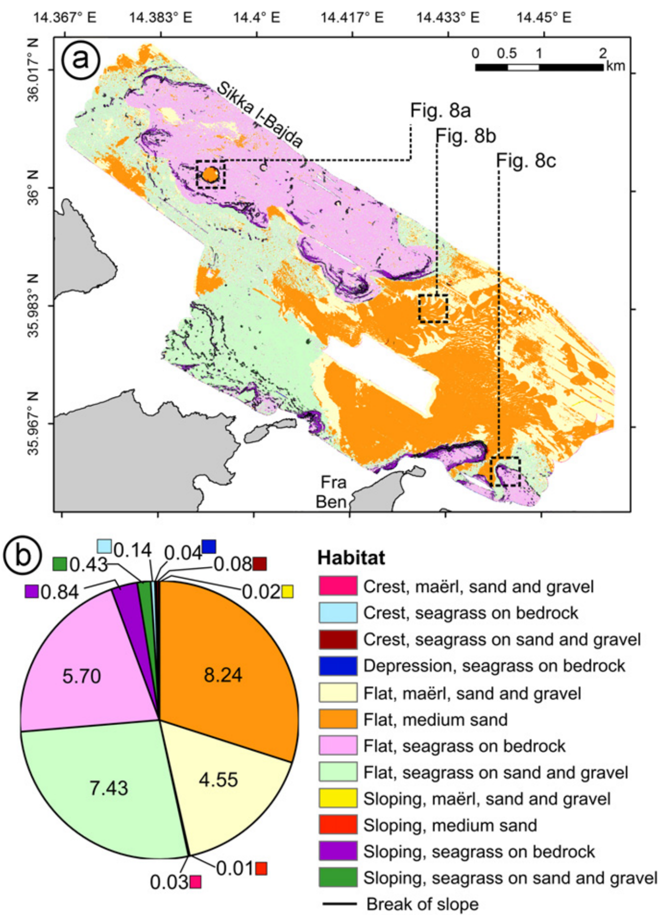

Fig. 7. (a) Habitat map generated by combining the topographic and seabed composition maps; (b) Pie chart of the areal fraction of each habitat across the study area (numbers denote coverage in km^2).

of the Sikka l-Bajda reef is interrupted by circular to elliptical depressions with steep walls that are filled with sand and gravel (Fig. 8(a)). We identify four of these structures on the Sikka l-Bajda reef and one offshore the Fra Ben peninsula to the south. The surface of Sikka l-Bajda reef is also characterised by pockets of sand, gravel and maërl. The reef is fringed by a narrow band of sloping terrain, which is interrupted in places by gently sloping terraces and steep escarpments. The escarpments located to the south-west of Sikka l-Bajda reef correspond to the boundaries of terraces that were not easily identifiable by visual interpretation.

5.2. Evaluation of the habitat mapping method

A visual assessment of the final habitat map provides the best test of the predictive accuracy for our method. We do this by comparing the ROV imagery and dive observations from the test sites, the locations of which are different from those of the training sites (Fig. 2(b)), with the classes plotted in our habitat map (Fig. 7).

For the most part, the mapped habitats coincide with the observations in the test sites (Fig. 9). Misclassification of habitats and linear artefacts occur occasionally, particularly where data are characterised by noise or gaps, which is not surprising. Since flat areas cover $>94\%$ of the study area, our test sites only cover these areas and we are not able to assess the performance of the method for other types of morphologies from ROV and dive imagery. However, as shown in Fig. 8, draping the habitat classes and breaks of slope on a 3D visualisation of the terrain shows that extracted elements coincide precisely with the features they are supposed to represent.

6. Discussion

In this paper we have outlined a semi-automated seafloor classification technique that transforms high-resolution MBES

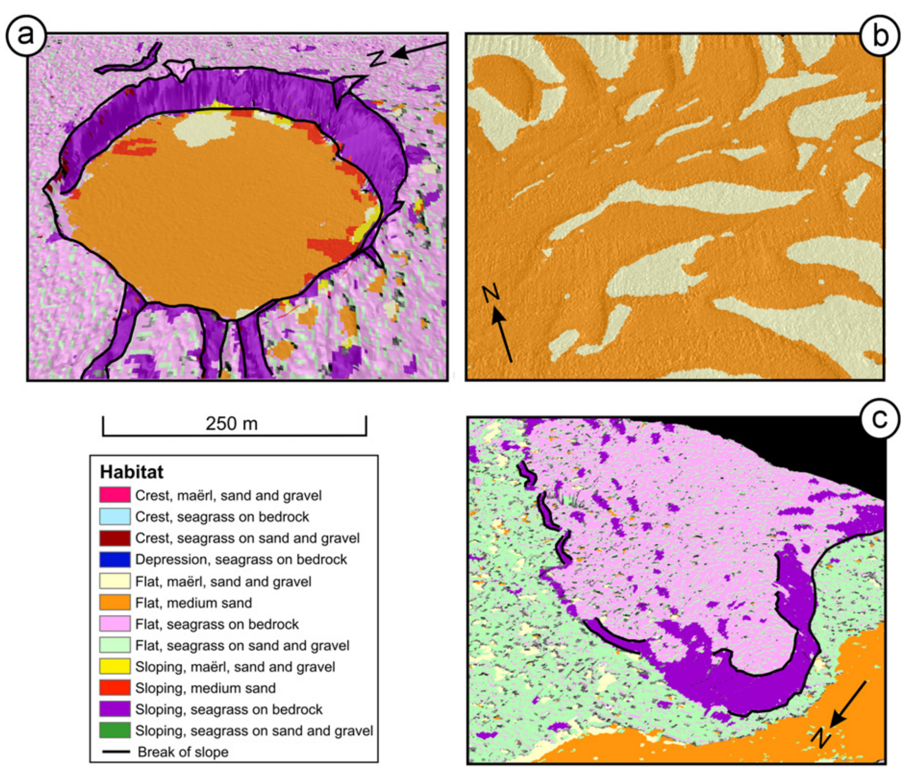

Fig. 8. Habitat map draped on 3D DEM for three sections from the habitat map: (a) Circular bedrock depression infilled with medium sediment; (b) Intricate pattern of lobes and ripples of medium sand overlying maërl associated with sand and gravel; (c) Submerged bedrock peninsula covered with seagrass and bordered by seagrass settled on sand and gravel. The location of these sections is denoted in Fig. 7(a).

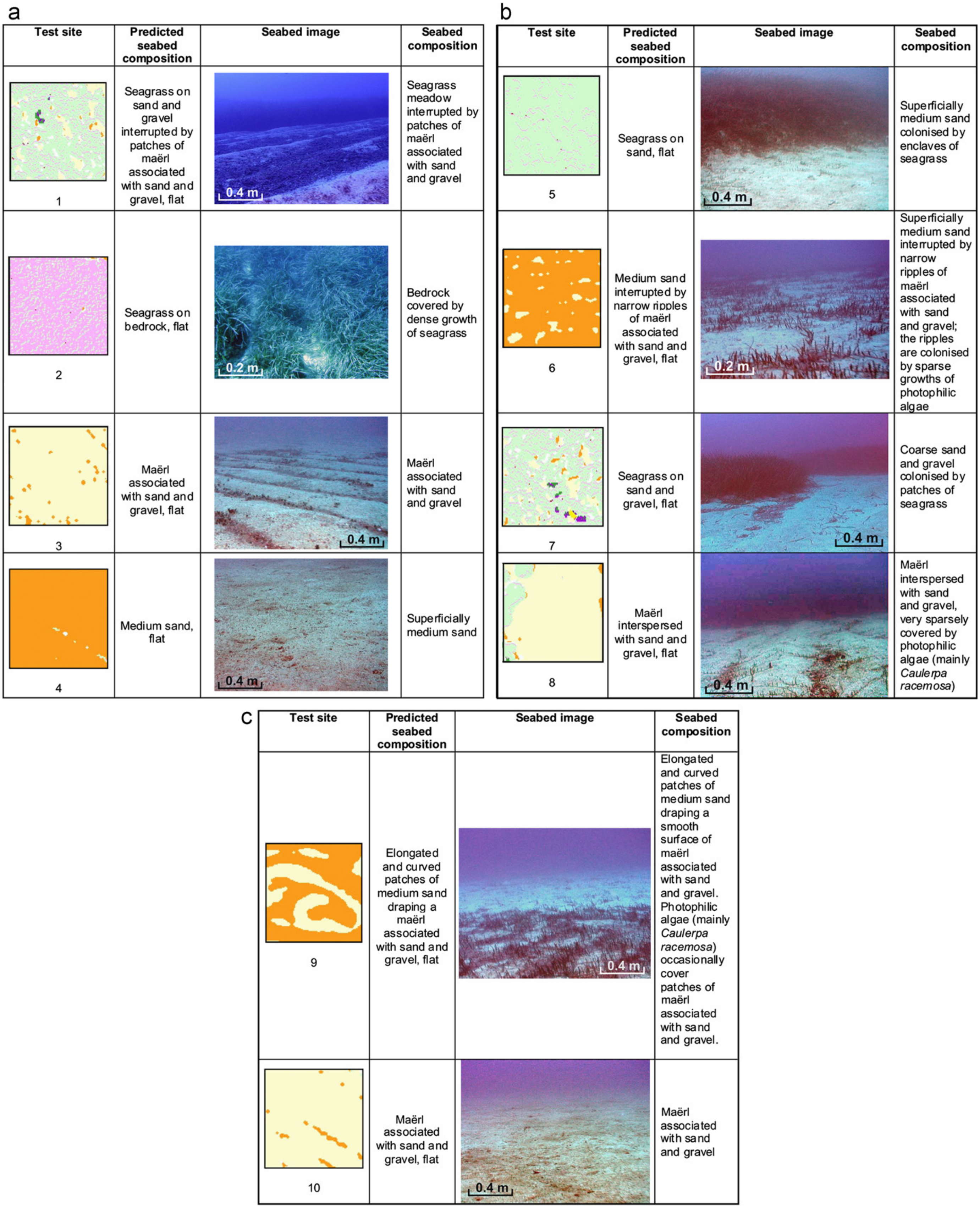

Fig. 9. Habitat description and predicted seabed composition (200 × 200 m; legend shown in Fig. 7), compared with ROV still imagery and interpreted seabed composition for test sites.

data, calibrated with seafloor imagery and samples, into meaningful habitats of distinct seafloor composition and morphology. By applying the methodology to bathymetric data collected from offshore the Maltese Islands we were able to identify five elementary morphological zones – flat and sloping zones, crests, depressions and breaks of slopes – using morphometric derivatives, BPI and geomorphometric mapping. Using the bathymetric data we were also able to discriminate between seagrass-covered and unvegetated seafloor on the basis of roughness. These two classes were further sub-divided into four habitats using supervised classification of morphometric derivatives (seagrass settled on sand and gravel, and seagrass settled on bedrock) and of backscatter data and their textures (medium sand, and maërl associated with sand and gravel). At the end we were able to segment the study area into twelve habitats (Fig. 7). The agreement of these mapped habitats with ROV imagery and dive observations lends credibility to the performance of our multi-method approach in segmenting the seafloor in the study area in a meaningful way.

In comparison to traditional methods of seafloor classification based on manual segmentation, our approach: (i) reduces operator bias and ensures consistency of classification results; (ii) causes negligible disturbance to the seabed; (iii) does not require considerable computer processing power, and it decreases the time and cost of data interpretation; (iv) is mainly implemented in a GIS environment, which allows further spatial and statistical analyses to be carried out. The MBES data used for this study have a grid dimension of 10^7 pixels, which is much larger than the 10^3 pixels of a typical computer screen. Such large volumes present a challenge to the effective exploitation of the data set by traditional visual interpretation. The spatial detail of our methodology, on the other hand, depends on the resolution of the MBES data rather than the extent of observation, which ensures that all the information generated by the MBES is utilised; this enhances the extraction and interpretation of topographic and seabed information.

The proposed approach can be applied to other shallow coastal areas around the world. The morphological zones identified by our method are universal and can be used to characterise the seafloor from any geological setting. The seabed composition classes are similar to the predominant seabed composition types in the Mediterranean region. Nevertheless, attention needs to be paid when using the method where seabed composition is significantly different; in this case, additional ground truth samples need to be gathered, although we recommend that this should be carried out prior to every new survey. Our method can be easily adapted to extract other types of morphology and composition not present in our study area (as shown by the versatility of geomorphometric techniques (Micallef et al., 2007) and textural analyses (Blondel, 1996)). The portability of our method is particularly enhanced by the use of textural indices, which are less system and site dependent. The thresholds proposed for the seabed morphological classification, on the other hand, need to be modified in case a coarser grid than that generated from our MBES data is employed (Evans, 1975).

Despite the fact that many recent studies have explored methods of automated classification of MBES data for the delineation of seafloor habitats (Brown and Blondel, 2009 + references therein; Che Hasan et al., 2012; Heap and Harris, 2011 + references therein; Shumchenia and King, 2010), a single technique for automated seabed classification that works well for all habitat types in all kinds of environments has never been devised. Our approach, in contrast to the above studies, builds on the premise that since seabed morphology and composition are so variable, the techniques used to classify them should be adaptable. What distinguishes our approach is the fact that we use a combination of techniques for bathymetric and backscatter data analyses to map specific types of morphologies and composition at various scales. The selection of the technique is based on identifying which geophysical parameter would be influenced by each seabed type under consideration, based on the characteristic that is most distinguishing. In comparison to some recent studies on the use of MBES for habitat mapping, the approach that we have proposed: (i) is simple and does not require specialised data processing (e.g., neural networks (Marsh and Brown, 2009)); (ii) distinguishes seagrass covered areas and classifies them on the basis of substrates (De Falco et al., 2010); and (iii) extracts geological lineaments and discontinuities, in addition to zones of similar habitats (Erdey-Heydorn, 2008).

In our method, backscatter data are shown to be an asset to seabed characterisation — they enhance the characterisation of fine scale structures that cannot be obtained from bathymetry alone, and the quality of the processed backscatter data is as good as those generated by side scan sonar. Our results confirm that backscatter intensity can be used as a proxy for sediment grain size, in accordance with many published studies (Collier and Brown, 2005; Edwards et al., 2003; Kostylev et al., 2005). Principal Component Analysis carried out for the backscatter, homogeneity and entropy data layers show that these parameters explain 93.1%, 5.7% and 1.2% of sediment grain size variability, respectively, in Fig. 6(c). Excluding homogeneity and entropy from the supervised classification in Section 4.2.3.1. results in higher noise and misclassification of habitats in some parts of the map, in comparison to Fig. 6(c). Therefore, although backscatter is the main characteristic determining segmentation of the study area into classes of medium sand and maërl associated with sand and gravel, including textural parameters in the classification improves the quality and reliability of backscatter classification, and the final habitat map overall.

Our method is semi-automated, and operator input is still necessary in the selection of the boundaries to spatially separate classes, in choosing the data layers to input in the classification technique and the classification method to be employed. Although this introduces a subjective component to the technique, we believe that expert input (e.g., in terms of regional knowledge of the seabed and how this would influence the geophysics on which the methodology is based) is an important parameter in our habitat mapping methodology that should not be excluded. A number of sources of error or uncertainty, analogous to those encountered in other seabed classification techniques, may also affect the accuracy of the final habitat map. Habitat misclassifications and artefacts, for example, coincided with noise or gaps in the multibeam data (Fig. 9), and ideally these should be kept to a minimum during data collection. The quality of the ground truthing samples has a significant bearing on the performance of supervised classification in our method, particularly with regards to segmentation of the seafloor by seabed composition; ground truthing data should thus be representative of all habitats in the study area. Spatial mismatch of ground truthing and hydroacoustic data is another potential source of error.

A further limitation of our method is the difficulty in discriminating between coarse sand and gravel from maërl associated with sand and gravel (e.g., the maërl beds mapped across the Sikka l-Bajda reef are likely to consist of sand and gravel only (Fig. 7)), or between *Posidonia oceanica* habitats with or without matte, due to the similar acoustic signature. The way to take forward our work in the near future will therefore be to improve the differentiation between different categories of the same habitat, for example by mapping the seafloor with MBES using different acoustic frequencies or beam level angular response.

7. Conclusions

The quantitative characterisation of MBES data for seafloor and habitat mapping is an advancing, but still underdeveloped, field that requires further research to realise the potential of the currently available MBES technology. In this study we demonstrate that the combination of high-resolution MBES bathymetry and backscatter data provides a robust means of producing detailed and accurate habitats maps of the shallow coastal waters of the Maltese Islands. Our approach consists of a semi-automated, GIS-based, multi-method system that combines a suite of geomorphometric and textural analytical techniques to map different types of seafloor morphologies and composition. Morphometric attributes, the Bathymetric Position Index and geomorphometric mapping are used to classify the seabed into five elementary morphological zones and features — flat and sloping zones, crests, depressions and breaks of slope. Subdivision of the seafloor into the four predominant types of composition – medium sand, maërl associated with sand and gravel, seagrass settled on sand and gravel, and seagrass settled on bedrock – was carried out using roughness estimation and supervised classifications of morphometric derivatives of the bathymetry and textural indices of backscatter; these were based on seafloor imagery and samples obtained from training stations. The resulting topographic and seabed composition maps were combined to plot the distribution of the predominant habitats in the coastal waters offshore NE Malta, some of which are of high conservation value. Ground-truthing of the habitat map by ROV imagery and dive observation confirms that our approach produces a simplified and accurate representation of seafloor habitats while using all the information available within MBES data sets. As the Government of Malta embarks on the mapping of its coastal waters in fulfillment of its obligations under the Maritime Strategy Directive, we expect that our approach can provide an efficient and cost-effective technique to map and manage Maltese coastal waters.

Acknowledgements

This research was supported by grant 398 of the Royal Institution of Chartered Surveyors (RICS) Education Trust, the University of Malta Research Fund 31-506 and Marie Curie Intra-European Fellowship PIEF-GA-2009-252702 within the 7th European Community Framework Programme. We kindly acknowledge RPM Nautical Foundation, the captain and crew of R/V Hercules, and Highland Geo Solutions for their assistance with data collection. Rut Pedrosa Pàmies is thanked for her assistance with granulometric analyses. We are grateful to the Hydrographic Office of the Malta Maritime Authority for providing access to bathymetric data of the Maltese coastal waters. The MBES, ROV video and dive surveys were possible following permits issued by the Malta Resources Authority and Environment Protection Directorate of the Malta Environment and Planning Authority.

References

Blondel, P., 1996. Segmentation of the Mid-Atlantic Ridge south of the Azores, based on acoustic classification of TOBI data. In: MacLeod, C.J., Tyler, P., Walker, C.L. (Eds.), Tectonic, Magmatic and Biological Segmentation of Mid-Ocean Ridges. Geological Society Special Publication, pp. 17–28.

Blondel, P., Parson, L.M., Robigou, V., 1998. TexAn: textural analysis of sidescan sonar imagery and generic seafloor characterisation. In: Oceans '98 IEEE/OES Conference Proceedings, Nice, France, pp. 419–423.

Blondel, P., 2000. Automatic mine detection by textural analysis of COTS sidescan sonar imagery. International Journal of Remote Sensing 21, 3115–3128.

Blondel, P., Gómez Sichi, O., 2009. Textural analyses of multibeam sonar imagery from Stanton Banks, Northern Ireland continental shelf. Applied Acoustics 70, 1288–1297.

Borg, J.A., Rowden, A.A., Attrill, M.J., Schembri, P.J., Jones, M.B., 2009. Occurrence and distribution of different bed types of seagrass *Posidonia oceanica* around the Maltese Islands. Mediterranean Marine Series 10, 45–61.

Borg, J.A., Schembri, P.J., 2002. Alignment of marine habitat data of the Maltese Islands to conform to the requirements of the EU habitats directive (Council Directive 92/43/EEC), p. 136.

Bosence, D.W.J., 1979. Live and dead faunas from coralline gravels. Co. Galway. Palaeontology 22, 449–478.

Boudouresque, C.F., Meinesz, A., 1982. Découverte de l'herbier de *Posidonies*. Port-Cros 4, 1–79.

Bourget, E., DeGuise, J., Daigle, G., 1994. Scales of substratum heterogeneity, structural complexity and the early establishment of a marine epibenthic community. Journal of Experimental Marine Biology and Ecology 181, 31–51.

Brown, C.J., Blondel, P., 2009. Developments in the application of multibeam sonar backscatter for seafloor habitat mapping. Applied Acoustics 70, 1242–1247.

Brown, C.J., Todd, B., Kostylev, J., Pickrill, R.A., V.E., 2011. Image-based classification of multibeam sonar backscatter data for objective surficial sediment mapping of Georges Bank, Canada. Continental Shelf Research 31, S110–S119.

Che Hasan, R., Ierodiaconou, D., Laurenson, L., 2012. Combining angular response classification and backscatter imagery segmentation for benthic biological habitat mapping. Estuarine, Coastal and Shelf Science 97, 1–9.

Cochrane, G.R., Lafferty, K.D., 2002. Use of acoustic classification of sidescan sonar data for mapping benthic habitat in the Northern Channel Islands, California. Continental Shelf Research 22, 683–690.

Collier, J.S., Brown, C.J., 2005. Correlation of sidescan backscatter with grain size distribution of surficial seabed sediments. Marine Geology 214, 431–449.

Cutter Jr., G.R., Rzhanov, Y., Mayer, L.A., 2003. Automated segmentation of seafloor bathymetry from multibeam echosounder data using local Fourier histogram texture features. Journal of Experimental Marine Biology and Ecology 285–286, 355–370.

Cusson, M., Bourget, E., 1997. Influence of topographic heterogeneity and spatial scales on the structure of the neighboring intertidal endobenthic macrofaunal community. Marine Ecology Progress Series 150, 181–193.

De Falco, G., Tonielli, R., Di Martino, G., Innangi, S., Simeone, S., Parnum, I.M., 2010. Relationship between multibeam backscatter, sediment grain size and *Posidonia oceanica* seagrass distribution. Continental Shelf Research 30, 1941–1950.

Edwards, B.D., Dartnell, P., Chezar, H., 2003. Characterizing benthic substrates of Santa Monica Bay with seafloor photography and multibeam sonar imagery. Marine Environmental Research 56, 47–66.

Erdey-Heydorn, M.D., 2008. An ArcGIS seabed characterization toolbox developed for investigating benthic habitats. Marine Geodesy 31, 318–358.

Evans, I.S., 1975. The Effect of Resolution on Gradients Calculated From an Altitude matrix, Report 3 on Grant ERO-591-73-G0040 'Statistical Characterisation of Altitude matrices by Computer. Department of Geography, University of Durham, Durham, p. 24.

Eyre, B.D., Maher, D., 2011. Mapping ecosystem processes and function across shallow seascapes. Continental Shelf Research 31, S162–S172.

Francour, P., Magreau, J.F., Mannoni, P.A., Cottalorda, J.M., Gratiot, J., 2006. Management guide for marine protected areas of the Mediterranean Sea. Universite´ de Nice-Sophia Antipolis & Parc National de Port-Cros, Nice, 68.

Freiwald, A., Beuck, L., Taviani, M., Hebbeln, D., 2009. R/V Meteor cruise M70-1 participants. The white coral community in the central Mediterranean Sea revealed by ROV surveys. Oceanography 22, 58–74.

Gao, D., Hurst, S.D., Karson, J.A., Delaney, J.R., Spiess, F.N., 1998. Computer-aided interpretation of side-looking sonar images from the eastern intersection of the Mid-Atlantic Ridge with the Kane Transform. Journal of Geophysical Research 103, 20997–21014.

Gray, J.S., 1997. Marine biodiversity: patterns, threats and conservation needs. Biodiversity and Conservation 6, 153–175.

Guichard, F., Bourget, E., 1998. Topographic heterogeneity, hydrodynamics and benthic community structure: a scale-dependent cascade. Marine Ecology Progress Series 171, 59–70.

Heap, A.D., Harris, P.T., 2011. Geological and biological mapping and characterisation of benthic marine environments — Introduction to the special issue. Continental Shelf Research 31, S1–S3.

Hemminga, M.A., Duarte, C.M., 2000. Seagrass Ecology. Cambridge University Press, Cambridge.

Jackson, D.R., Richardson, M.D., 2007. High-Frequency Seafloor Acoustics. Springer, London.

Jackson, J.B.C., Kirby, M.X., Berger, W.H., Bjorndal, K.A., Botsford, L.W., Bourque, B.J., Bradbury, R.H., Cooke, R., Erlandson, J., Estes, J.A., Hughes, T.P., Kidwell, S., Lange, C.B., Lenihan, H.S., Pandolfi, J.M., Peterson, C.H., Steneck, R.S., Tegner, M.J., Warner, R.R., 2001. Historical overfishing and the recent collapse of coastal ecosystems. Science 293, 629–638.

Kenny, A.J., Cato, I., Desprez, M., Fader, G.B., Schuttenhelm, R.T.E., Side, J., 2003. An overview of seabed-mapping technologies in the context of marine habitat classification. ICES Journal of Marine Science 60, 411–418.

Kostylev, V.E., Courtney, R.C., Robert, G., Todd, B.J., 2003. Stock evaluation of giant scallop (*Placopecten magellanicus*) using high-resolution acoustic for seabed mapping. Fisheries Research 60, 479–492.

Kostylev, V.E., Todd, B., Fader, J., Courtney, G.B., Cameron, R.C., Pickrill, R.A., G.D., 2001. Benthic habitat mapping on the Scotian Shelf based on multibeam

bathymetry, surficial geology and seafloor photographs. Marine Ecology Progress Series 219, 121–137.
Kostylev, V.E., Todd, B.J., Longva, O., Valentine, P.C., 2005. Characterization of benthic habitat on northeastern Georges Bank, Canada. Benthic Habitats and the Effects of Fishing 41, 141–152.
Lamarche, G., Lurton, X., Verdier, A.-L., Augustin, J.-M., 2011. Quantitative characterisation of seafloor substrate and bedforms using advanced processing of multibeam backscatter—application to Cook Strait, New Zealand. Continental Shelf Research 31, S93–S109.
Le Bas, T.P., Hühnerbach, V., 1998. PRISM processing of remotely-sensed imagery for seafloor mapping handbook. Southampton Oceanography Centre, 82.
Le Bas, T.P., Huvenne, V.A.I., 2009. Acquisition and processing of backscatter data for habitat mapping: comparison of multibeam and sidescan systems. Applied Acoustics 70, 1248–1257.
Lundblad, E., Wright, D.J., Miller, J.P., Larkin, E.M., Rinehart, R., Battista, T., Anderson, S.M., Naar, D.F., Donahue, B.T., 2006. A benthic terrain classification scheme for American Samoa. Marine Geodesy 29, 89–111.
Marsh, I., Brown, C., 2009. Neural network classification of multibeam backscatter and bathymetry data from Stanton Bank (Area IV). Applied Acoustics 70, 1269–1276.
McGonigle, C., Brown, C., Quinn, R., Grabowski, J., 2009. Evaluation of image-based multibeam sonar backscatter classification for benthic habitat discrimination and mapping at Stanton Banks, UK. Estuarine, Coastal and Shelf Science 81, 423–437.
Micallef, A., Berndt, C., Debono, G., 2011. Fluid flow systems of the Malta Plateau, central Mediterranean Sea. Marine Geology 284, 74–85.
Micallef, A., Berndt, C., Masson, D.G., Stow, D.A.V., 2007. A technique for the morphological characterization of submarine landscapes as exemplified by debris flows of the Storegga Slide. Journal of Geophysical Research 112, F02001.
Mitchell, N.C., Clarke, J.E.H., 1994. Classification of seafloor geology using multibeam sonar data from the Scotian Shelf. Marine Geology 121, 143–160.
Pedley, H.M., House, M.R., Waugh, B., 1976. The geology of Malta and Gozo. Proceedings of the Geologists' Association 87, 325–341.
Pérès, J.M., Picard, J., 1964. Nouveau manuel de bionomie benthique de la Mer Méditerranée. Recueil des travaux de la Station Marine d'Endoume 31, 5–137.
Pergent-Martini, C., Le Ravallec, C., 2007. Guidelines for impact assessment on seagrass meadows, United Nations Environment Programme – Regional Activity Centre for Specially Protected Areas (RAC/SPA), Tunis, Tunisia, p. 48.
Reed, T.B., Hussong, D., 1989. Digital image processing techniques for enhancement and classification of SeaMARC II sidescan sonar imagery. Journal of Geophysical Research 94, 7469–7490.
Reuther, C.D., Eisbacher, G.H., 1985. Pantelleria rift-crustal extension in a convergent intraplate setting. Geologische Rundschau 74, 585–597.
Sciberras, M., Rizzo, M., Mifsud, J.R., Camilleri, K., Borg, J.A., Lanfranco, E., Schembri, P.J., 2009. Habitat structure and biological characteristics of a maërl bed off the northeastern coast of the Maltese Islands (central Mediterranean). Marine Biodiversity 39, 251–264.
Shokr, M., 1991. Evaluation of second-order texture parameters for sea ice classification from radar images. Journal of Geophysical Research 96, 10625–10640.
Shumchenia, E.J., King, J.W., 2010. Comparison of methods for integrating biological and physical data for marine habitat mapping and classification. Continental Shelf Research 30, 1717–1729.
Singh, H., Adams, J., Mindell, D., Foley, D., 2000. Imaging underwater for archaeology. Journal of Field Archaeology 27, 319–328.
Smith, W.H.F., Sandwell, D.T., 1997. Global seafloor topography from satellite altimetry and ship depth soundings. Science 277, 1957–1962.
Snelgrove, P.V.R., Butman, C.A., 1994. Animal-sediment relationships revisited: cause versus effects. Oceanography and Marine Biology Annual Review 32, 111–177.
Todd, B.J., Fader, G.B.J., Courtney, R.C., Pickrill, R.A., 1999. Quaternary geology and surficial sediment processes: Browns Bank, Scotian Shelf, based on multibeam bathymetry. Marine Geology 162, 165–214.
Weiss, A.D., 2001. Topographic positions and landforms analysis, ESRI International User Conference, San Diego, California.
Wentworth, C.K., 1922. A scale of grade and class terms for clastic sediments. The Journal of Geology 30, 377–392.
Wright, D.J., Heyman, W.D., 2008. Introduction to the special issue: marine and coastal GIS for geomorphology, habitat mapping and marine reserves. Marine Geodesy 31, 223–230.